

Scalar flux spectrum in isotropic steady turbulence with a uniform mean gradient

Takeshi Watanabe^{a)} and Toshiyuki Gotoh^{b)}

Department of Engineering Physics, Graduate School of Engineering, Nagoya Institute of Technology, Gokiso, Showa-ku, Nagoya 466-8555, Japan and CREST, Japan Science and Technology Agency, 4-1-8 Honcho, Kawaguchi, Saitama 332-0012, Japan

(Received 10 August 2007; accepted 13 November 2007; published online 18 December 2007)

The scaling law of a scalar flux spectrum (velocity-scalar cospectrum) in the inertial convective range of passive scalar turbulence under a uniform mean scalar gradient is examined using direct numerical simulation with a resolution of up to 2048^3 grid points. When the Reynolds number Re_λ is increased up to $Re_\lambda=585$, the scalar flux spectrum tends to obey the power law $k^{-7/3}$, as predicted by Lumley [J. Atmos. Sci. **21**, 99 (1964); Phys. Fluids **10**, 855 (1967)], with a nondimensional constant of $C_{u\theta}=1.50\pm 0.08$ at $Re_\lambda=585$. The Re_λ effect on the scaling of the scalar flux spectrum is well compensated using the mean molecular destruction of the scalar flux $\bar{\epsilon}_{u\theta}$. The Re_λ dependence of $C_{u\theta}$ is also compared with the results of previous studies, and its asymptotic state at an infinite Reynolds number is discussed. © 2007 American Institute of Physics.

[DOI: 10.1063/1.2821906]

Passive scalars advected by turbulence have been investigated with great interest, not only because of their importance in industrial and/or environmental contexts, but also due to their peculiar nature that can be used to elucidate the dynamics and statistics of turbulence.¹ In many cases, an imposed mean scalar gradient works as a source of scalar fluctuations and plays an important role in the formation of ramp-cliff structures, which cause strong intermittency and persistent anisotropy at small-scales.^{1,2} One of the key quantities is the scalar flux (velocity-scalar cross-correlation) $\langle u_3\theta \rangle$, which has a finite value when a mean scalar gradient exists in the x_3 direction. The scalar flux spectrum $E_{u\theta}(k)$ is a measure of how the scalar flux is distributed over the scales, and is defined by $-\langle u_3\theta \rangle = \int_0^\infty E_{u\theta}(k) dk$ when $\langle u_3\theta \rangle$ is negative, i.e., $E_{u\theta}(k) = -\int dS_k \langle u_3(\mathbf{k})\theta(-\mathbf{k}) \rangle$, where the integral $\int dS_k$ is taken over a spherical shell in the wavenumber space.

The scaling behavior of the scalar flux spectrum in the inertial convective range (ICR) was first predicted by Lumley^{3,4} on dimensional grounds as

$$E_{u\theta}(k) = C_{u\theta} G \bar{\epsilon}^{-1/3} k^{-7/3}, \quad (1)$$

where G is the mean scalar gradient [$\mathbf{G}=(0,0,G)$], $\bar{\epsilon}$ is the mean dissipation rate of the kinetic energy, and $C_{u\theta}$ is a nondimensional constant expected to be of order unity. Motivated by the scaling of $E_{u\theta}(k)$ using the Kolmogorov theory and by practical importance of giving an estimate of the eddy diffusivity $K_{\text{eddy}} = -\langle u_3\theta \rangle / G$, many studies have been made for the scalar flux spectrum with a mean gradient.⁵⁻¹⁴ Theoretical studies using the eddy damped quasilinear Markovian (EDQNM) model have shown that in the ICR $E_{u\theta}(k) \propto k^{-2}$ for low to moderate and Lumley's scaling law [Eq. (1)] is approached only when $Re_\lambda = O(10^7)$.^{9,11} This feature has been observed also in experimental studies of grid

turbulence,^{5,6} in which the spectral slope of the one-dimensional (1-D) scalar flux spectrum approaches the power law form close to k^{-2} with increasing Re_λ up to $Re_\lambda=582$. Recent experimental measurements in a turbulent jet observed both $k^{-7/3}$ and k^{-2} for the axial or radial velocity components.¹³ Earlier observations consistent or inconsistent with Eq. (1) are also described in Refs. 10 and 11. Scalar flux spectra that are less steep than Eq. (1) have been reported also in direct numerical simulations^{9,10} (DNSs) and large eddy simulation,¹⁰ but the width of the ICR due to computational limitation was not long enough to reach definite conclusion on the spectral slope.

The above facts show that there is no conclusive agreement on the scaling of the scalar flux spectrum, suggesting that the scaling law should be carefully examined when Re_λ is low to moderate or finite. Indeed, in DNS, for example, a resolution of at least 1024^3 is required to obtain an ICR with a reasonable degree of accuracy to distinguish from other scaling ranges and/or the spectral bump.¹⁵⁻¹⁹ To observe Eq. (1), it is necessary to achieve a much higher Re_λ than required to observe the 5/3 law for the energy and scalar variance spectra.^{5,6,10,11} In order to address the above problem, we have done very high resolution DNSs with grid points up to 2048^3 for the passive scalar turbulence with a mean scalar gradient, and examined Lumley's scaling law (1) for the scalar flux spectrum at $Re_\lambda=585$, which is higher than in previously reported studies.^{7,9,10,14}

The governing equation for the scalar field $\theta(\mathbf{x},t)$ is given by $(\partial_t + u_j \partial_j) \theta = \kappa \partial_j^2 \theta - Gu_3$, where the incompressible velocity field $u_i(\mathbf{x},t)$ obeys the Navier-Stokes equation $(\partial_t + u_j \partial_j) u_i = -\partial_i P + \nu \partial_j^2 u_i + f_i$ with $\partial_i u_i = 0$. The coefficients ν and κ are the kinematic viscosity and molecular diffusivity, respectively. The Schmidt number $Sc = \nu / \kappa$ was fixed at unity in the simulations. The random force f_i was solenoidal, Gaussian white in time, and applied in the low wavenumber band.¹⁵ This forcing mechanism is appropriate to maintain

^{a)}Electronic mail: watanabe@nitech.ac.jp.

^{b)}Electronic mail: gotoh.toshiyuki@nitech.ac.jp.

TABLE I. Fundamental DNS parameters obtained by the present series of DNSs, where the Taylor microscale Reynolds number Re_λ , and the normalized dissipations for the kinetic energy $\hat{\epsilon}$, scalar variance $\hat{\chi}$, and scalar flux $\hat{\epsilon}_{u\theta}$ are defined by $Re_\lambda = u_{rms}\lambda/\nu$, $\hat{\epsilon} = \bar{\epsilon}L/u_{rms}^3$, $\hat{\chi} = \bar{\chi}L/u_{rms}\theta_{rms}^2$, and $\hat{\epsilon}_{u\theta} = \bar{\epsilon}_{u\theta}/G(u_{rms}^2)$, respectively. The steady-state statistical average is taken over space and time during the normalized averaging time T_{av} using the large eddy turnover time $T_{eddy} = L/u_{rms}$ and denoted by $\langle \dots \rangle$.

	Run G1	Run G2	Run G3	Run G4
N	256	512	1024	2048
$K_{max}\bar{\eta}$	1.0	1.1	1.1	1.4
Re_λ	174	263	468	585
T_{av}	27	5.6	4.0	1.2
$\hat{\epsilon}$	0.482	0.468	0.444	0.462
$\hat{\chi}$	0.379	0.378	0.402	0.444
$\hat{\epsilon}_{u\theta}$	0.069	0.050	0.031	0.027

the Reynolds numbers high and to realize the isotropic velocity field even near the forcing scales, leading to the inertial range wider than that by decaying turbulence case. A uniform mean scalar gradient was imposed in the x_3 direction and fixed as $G=1$. The DNS numerical scheme was unchanged from the previous studies.^{20,21} We performed DNSs for different Re_λ cases. The numerical conditions and DNS parameters are summarized in Table I. The present DNSs satisfied the required accuracy conditions as far as the statistics of the convection-dominated scaling range are concerned.^{17,18}

To confirm the existence of an ICR, the kinetic energy and scalar variance spectra compensated using Kolmogorov–Obukhov–Corrsin scaling, i.e., $\hat{E}(k\bar{\eta}) = \bar{\epsilon}^{-2/3}k^{5/3}E(k)$ and $\hat{E}_\theta(k\bar{\eta}) = \bar{\chi}^{-1}\bar{\epsilon}^{1/3}k^{5/3}E_\theta(k)$, are shown in Fig. 1 for all runs, where $\bar{\chi}$ is the mean dissipation rate for the scalar variance. The curves fell almost on a single curve, irrespective of Re_λ , for both $E(k)$ and $E_\theta(k)$. This suggests that we can obtain well converged second-order moments, even when the averaging time is insufficient, as is the case for run G4. When

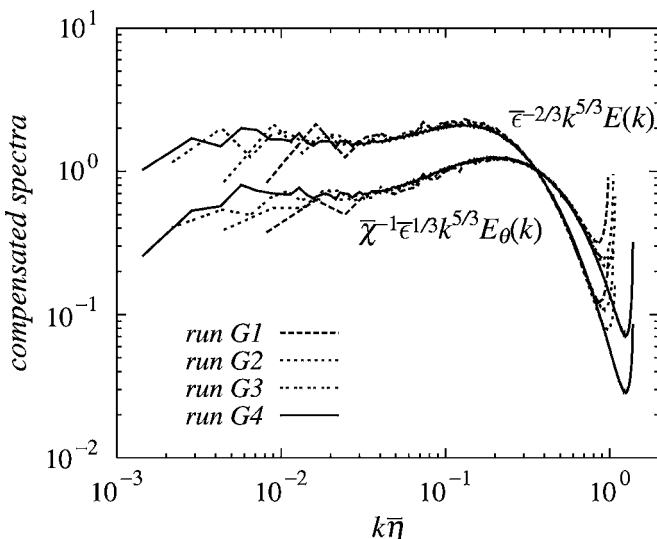


FIG. 1. Variations of the compensated spectra for the energy and scalar variance $\hat{E}(k\bar{\eta}) = \bar{\epsilon}^{-2/3}k^{5/3}E(k)$ and $\hat{E}_\theta(k\bar{\eta}) = \bar{\chi}^{-1}\bar{\epsilon}^{1/3}k^{5/3}E_\theta(k)$ against Re_λ .

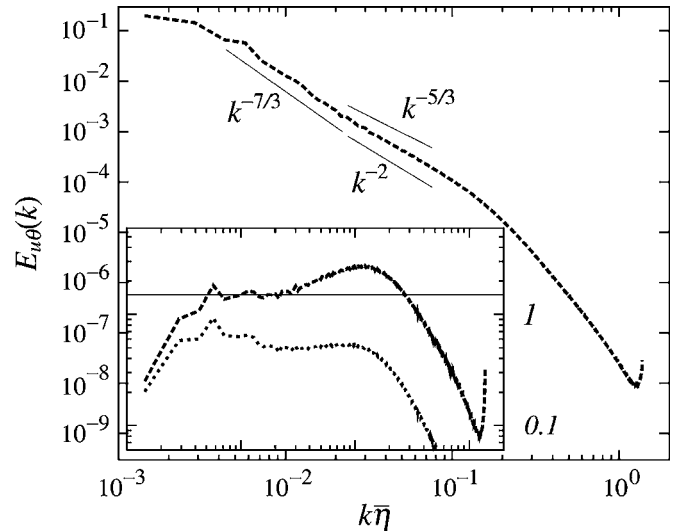


FIG. 2. Shell-summed scalar flux spectrum $E_{u\theta}(k)$ obtained from run G4. The thin reference lines correspond to the power law forms for $k^{-7/3}$, k^{-2} and $k^{-5/3}$. The inset plot gives the behavior of the compensated $E_{u\theta}(k)$ in terms of Lumley's scaling $G^{-1}\bar{\epsilon}^{-1/3}k^{7/3}E_{u\theta}(k)$ (upper curve) and $k^2E_{u\theta}(k)$ (lower curve), respectively. The horizontal thin line in the inset represents the value of 1.50, which was obtained by averaging the values of the compensated spectrum over $0.0085 \leq k\bar{\eta} \leq 0.023$.

Re_λ increases, the flat range in the scale $k\bar{\eta} < 0.03$ extends slowly toward the smaller wavenumbers. Plateaus are observed in the range $0.003 < k\bar{\eta} < 0.03$ of run G4, although the spectral slopes are slightly steeper than $k^{-5/3}$, as discussed later. The Kolmogorov and Obukhov–Corrsin constants are roughly evaluated as $K \approx 1.61$ and $C_{oc} \approx 0.68$, respectively, which are in good agreement with the values obtained by a passive scalar DNS with an isotropic random source²¹ and the experimental values $C_{oc}^{1D} \approx 0.4$ ($C_{oc} = 5C_{oc}^{1D}/3 \approx 0.67$) obtained by Sreenivasan,²² who carefully examined the values reported in many experiments.

Figure 2 shows the behavior of $E_{u\theta}(k)$ obtained from run G4. Scaling law close to the form $k^{-7/3}$ is observed in the range $0.004 < k\bar{\eta} < 0.03$, which is well within the ICR of $E(k)$ and $E_\theta(k)$ (Fig. 1). In the range of $0.03 < k\bar{\eta} < 0.1$, we observe another scaling law of $E_{u\theta}(k)$ between k^{-2} and $k^{-5/3}$. To more carefully examine the scaling behavior, the compensated plots $G^{-1}\bar{\epsilon}^{-1/3}k^{7/3}E_{u\theta}(k)$ and $k^2E_{u\theta}(k)$ are simultaneously shown in the inset of the figure. The scaling of $E_{u\theta}(k) \propto k^{-7/3}$ can be clearly seen in the range $0.006 < k\bar{\eta} < 0.03$. The spectral bump is manifested in the high wavenumber range of $0.03 < k\bar{\eta} < 0.1$ as well as for $E(k)$ and $E_\theta(k)$; the peak wavenumber of the bump is approximately $k_p\bar{\eta} \approx 0.11$, which is comparable to that of $E(k)$ ($k_p\bar{\eta} = 0.13$) and smaller than that of $E_\theta(k)$ ($k_p\bar{\eta} = 0.2$). The inset of the Fig. 2 indicates that the scaling behavior in the range of $0.03 < k\bar{\eta} < 0.1$ is closer to k^{-2} rather than $k^{-5/3}$, and suggests that this scaling behavior corresponds to the spectral behavior $E_{u\theta}(k) \propto k^{-2}$ observed in the previous studies, although we are still far from definite conclusion and further studies with higher Re_λ are necessary.

The nondimensional constant $C_{u\theta}$ for Lumley's scaling (1) was $C_{u\theta} = 1.50 \pm 0.08$, which was obtained by computing the mean and standard deviation of the fluctuations of the

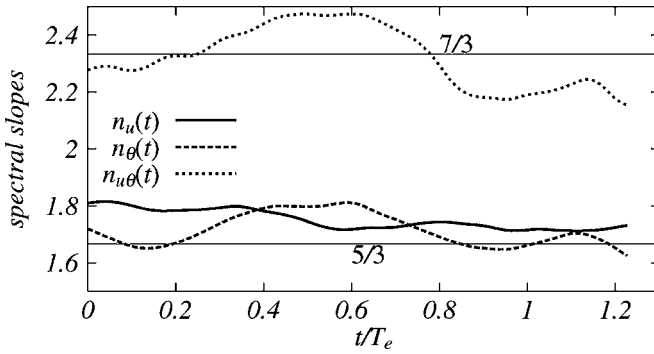


FIG. 3. Temporal variations in the scaling exponents of the spectra $E(k, t)$, $E_\theta(k, t)$, and $E_{u\theta}(k, t)$, evaluated in the ICR of $0.0085 \leq k\bar{\eta} \leq 0.023$, obtained from the instantaneous fields of run G4. The horizontal thin lines indicate the values from the dimensional analysis. The mean values of the spectral slopes averaged over the duration of the temporal fluctuations are $\langle n_u \rangle_t = 1.75 \pm 0.04$, $\langle n_\theta \rangle_t = 1.72 \pm 0.06$, and $\langle n_{u\theta} \rangle_t = 2.32 \pm 0.11$, where the errors denote the standard deviations due to the temporal fluctuations.

compensated spectrum in the range $0.0085 \leq k\bar{\eta} \leq 0.023$. The constant $C_{u\theta} = 3.5$ by the spectral closure in Ref. 9 is considerably larger than 1.5 by the present DNS, while $C_{u\theta} \approx 1.2$ by the EDQNM model from Fig. 8 in Ref. 11 when $Re_\lambda = 10^7$.

We investigated the temporal variations of the spectral slopes to determine the degree of robustness of the $7/3$ law observed in Fig. 2. We define the instantaneous scaling exponent $n_{u\theta}(t)$ by $E_{u\theta}(k, t) \sim k^{-n_{u\theta}(t)}$ within the ICR. Figure 3 shows the temporal variations of the exponents for the energy $n_u(t)$, scalar variance $n_\theta(t)$, and scalar flux $n_{u\theta}(t)$ obtained from run G4. The value of $n_{u\theta}(t)$ varies with time around the predicted value of $7/3$, while $n_u(t)$ and $n_\theta(t)$ fluctuate above $5/3$. The mean values and standard deviations with respect to the temporal fluctuations are $\langle n_u \rangle_t = 1.75 \pm 0.04$, $\langle n_\theta \rangle_t = 1.72 \pm 0.06$, and $\langle n_{u\theta} \rangle_t = 2.32 \pm 0.11$. Thus, the mean value of $n_{u\theta}$ is close to $7/3$, although the standard deviation of $n_{u\theta}$ is larger than those of n_u and n_θ . The value of $\langle n_{u\theta} \rangle_t = 1.75$ deviated from the dimensional prediction by $1.75 - 1.67 = 0.08$, which is comparable to observations at a higher Re_λ DNS¹⁶ and atmospheric measurements.²³

The 1-D scalar flux spectrum is usually examined in experimental studies and defined by $E_{u\theta}^{1T}(k_1) \equiv -\int \int_{-\infty}^{\infty} dk_2 dk_3 \langle u_3(\mathbf{k}) \theta(-\mathbf{k}) \rangle$ (transverse) or $E_{u\theta}^{1L}(k_3) \equiv -\int \int_{-\infty}^{\infty} dk_1 dk_2 \langle u_2(\mathbf{k}) \theta(-\mathbf{k}) \rangle$ (longitudinal). Its relationship to $E_{u\theta}(k)$ is⁸

$$E_{u\theta}^{1L}(k_3) = \frac{3}{4} \int_{k_3}^{\infty} \frac{k^2 - k_3^2}{k^3} E_{u\theta}(k) dk, \quad (2)$$

where $E_{u\theta}^{1T}(k)$ is usually observed in experimental studies and $E_{u\theta}^{1T}(k) = -(k^2/2)(d/dk)E_{u\theta}^{1L}(k)/k$ must be satisfied from the result in Ref. 8. Figure 4 shows the variation in the compensated scalar flux spectrum $G^{-1}\bar{\epsilon}^{-1/3}k_3^{7/3}E_{u\theta}^{1L}(k_3)$ for various Re_λ , where $E_{u\theta}^{1L}(k_3)$ is computed directly according to its definition instead of using Eq. (2). The flat range of the ICR slowly extends toward smaller wavenumbers with increasing Re_λ . The mean value of the compensated spectrum in this plateau was evaluated using the relationship given by Eq. (2) as $C_{u\theta}^{1L} = 27C_{u\theta}/182 = 0.22$ when $C_{u\theta} = 1.5$. The curves for various Re_λ do not collapse well, even in the near dissipation

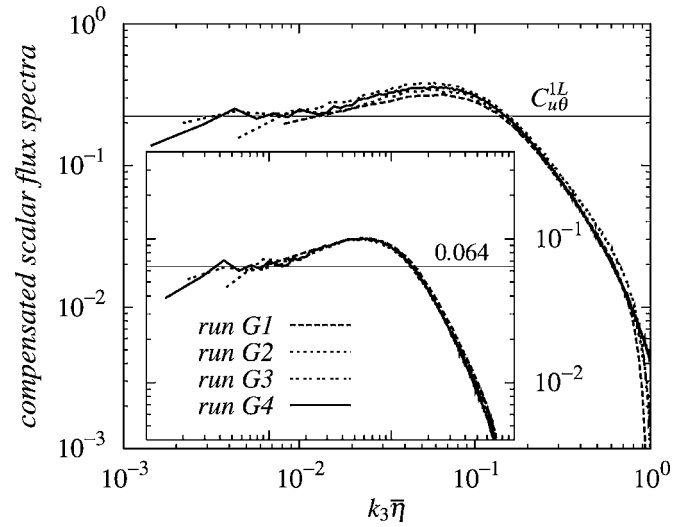


FIG. 4. Variation in the compensated 1-D scalar flux spectra in terms of Lumley's scaling $G^{-1}\bar{\epsilon}^{-1/3}k_3^{7/3}E_{u\theta}^{1L}(k_3)$ against Re_λ . The horizontal thin line represents the constant evaluated using Eqs. (1) and (2) with $C_{u\theta} = 1.5$. Inset: Variation in the function $G^{-1}\bar{\epsilon}^{-1/3}k_3^{7/3}E_{u\theta}^{1L}(k_3)/A(Re_\lambda) \equiv \bar{\epsilon}_{u\theta}(\bar{\epsilon}\bar{\eta})^{-2/3}G^{-1}$ for various Re_λ . The collapse of the curves compares satisfactorily to the usual compensated form.

range, which is in contrast to the excellent collapse for both the energy and scalar variance spectra shown in Fig. 1. This trend has been observed in previous DNS studies,⁹ emphasizing the sensitivity of the small-scale statistics of the scalar flux on the large- and small-scale conditions. This situation is also similar to that of the pressure spectrum, which has a $k^{-7/3}$ scaling in the inertial range and depends slightly on Re_λ , even in the dissipation range.²⁴

The results shown in Fig. 4 suggest that the scalar flux spectrum obeys the scaling law

$$E_{u\theta}^{1L}(k_3) = C_1(Re_\lambda)G\bar{\epsilon}^{1/3}k_3^{-7/3}f(k_3\bar{\eta}), \quad (3)$$

where $f(x)$ is a nondimensional function supposed to be Re_λ independent and satisfying $f(0) = 1$, and $C_1(Re_\lambda)$ is a constant dependent on Re_λ . The constant $C_1(Re_\lambda)$ is expressed in terms of the average rate of the molecular destruction of the scalar flux defined by $\bar{\epsilon}_{u\theta} = (\nu + \kappa) \int_0^\infty k^2 E_{u\theta}(k) dk$, which represents the statistics of the scalar flux at small scales. Substituting Eq. (3) in the definition of $\bar{\epsilon}_{u\theta}$ yields $C_1(Re_\lambda) = (\bar{\epsilon}\bar{\eta})^{-2/3}\bar{\epsilon}_{u\theta}/(GD_1)$ with $D_1 \equiv [10(1+S_c^{-1})] \int_0^\infty x^{-1/3}f(x)dx$. The function $f(k_3\bar{\eta})/D_1 = G^{-1}\bar{\epsilon}^{-1/3}k_3^{7/3}E_{u\theta}^{1L}(k_3)/A(Re_\lambda)$ with $A(Re_\lambda) \equiv \bar{\epsilon}_{u\theta}(\bar{\epsilon}\bar{\eta})^{-2/3}G^{-1}$ for various Re_λ is plotted in the inset of Fig. 4. Collapse of the curves is improved within the Reynolds numbers and wavenumbers studied here.

We now examine the Re_λ dependence of the nondimensional constant $C_{u\theta}$. The scaling form [Eq. (3)] with $k\bar{\eta} \ll 1$ leads to $C_{u\theta}^{1L} = C_1(Re_\lambda) \propto \hat{\epsilon}_{u\theta} Re_\lambda$ using $Re_\lambda \equiv \sqrt{15}\hat{\epsilon}^{-2/3}(L/\bar{\eta})^{2/3}$, where $\hat{\epsilon} \equiv \bar{\epsilon}L/u_{rms}^3$ and $\hat{\epsilon}_{u\theta} \equiv \bar{\epsilon}_{u\theta}/Gu_{rms}^2$; L is the integral scale. The DNS and EDQNM closure computations indicate that $\hat{\epsilon}_{u\theta}$ varies with Re_λ as $\hat{\epsilon}_{u\theta} \propto Re_\lambda^{-\delta}$ with $\delta \approx 0.77$ in the range $30 \leq Re_\lambda \leq 300$ (Refs. 7 and 11) or $\delta \approx 1$ in the range $Re_\lambda > 10^3$.¹¹ Grid turbulence experiments have suggested $\delta = 0.7 - 0.9$ in the range $85 \leq Re_\lambda \leq 582$.⁶ The present DNS gives $\hat{\epsilon}_{u\theta} = 3.9Re_\lambda^{-0.78}$, which was obtained by

fitting the data from Table I. Therefore, $C_{u\theta}$ depends on Re_λ as $C_{u\theta} \propto Re_\lambda^{1-\delta}$, indicating a slightly increasing function of Re_λ in the range $Re_\lambda < O(10^3)$ since $\delta=0.78$.

If an asymptotic state free of Re_λ is realized for infinite Reynolds numbers, then $\hat{\epsilon}_{u\theta} \propto Re_\lambda^{-1}$,¹¹ meaning that $\hat{\epsilon}_{u\theta}$ must vanish. Present study suggests that even when the scaling exponent 7/3 is observed at moderate Re_λ , the universality of the scalar flux spectrum ($C_{u\theta}$) would be attained at much larger Re_λ .

In summary, we examined the scaling law of the scalar flux spectrum in the ICR of passive scalar turbulence with a uniform mean scalar gradient using a high resolution DNS with 2048^3 grid points. The scaling law predicted by Lumley^{3,4} was observed when Re_λ was increased up to $Re_\lambda = 585$. Lumley's nondimensional constant, evaluated numerically, was $C_{u\theta} = 1.50 \pm 0.08$. We showed that the Re_λ effect on the scalar flux spectrum was well compensated using $\bar{\epsilon}_{u\theta}$. This also means that $C_{u\theta}$ depends on Re_λ when Re_λ is low to moderate. It is indispensable to perform higher Re_λ DNSs to obtain definite answer to the scaling of the scalar flux spectrum and the universality of the constant $C_{u\theta}$.

We thank the Earth Simulator Center, the Theory and Computer Simulation Center of the National Institute for Fusion Science, and the Information Technology Center of Nagoya University for providing the computational resources.

T.W. was supported by the Tatematsu Foundation and by Grant-in-Aid for Scientific Research No. 17760139 from the Ministry of Education, Culture, Sports, Science and Technology of Japan. T.G.'s work was supported by Grant-in-Aid for Scientific Research No. 19560168-0 from the Ministry of Education, Culture, Sports, Science and Technology of Japan.

¹Z. Warhaft, "Passive scalars in turbulent flows," *Annu. Rev. Fluid Mech.* **32**, 203 (2000).

²B. I. Shraiman and E. D. Siggia, "Scalar turbulence," *Nature (London)* **405**, 639 (2000).

³J. L. Lumley, "The spectrum of nearly inertial turbulence in a stably stratified fluid," *J. Atmos. Sci.* **21**, 99 (1964).

⁴J. L. Lumley, "Similarity and the turbulent energy spectrum," *Phys. Fluids* **10**, 855 (1967).

⁵L. Mydlarski and Z. Warhaft, "Passive scalar statistics in high-Péclet-number grid turbulence," *J. Fluid Mech.* **358**, 135 (1998).

⁶L. Mydlarski, "Mixed velocity-passive scalar statistics in high-Reynolds-number turbulence," *J. Fluid Mech.* **475**, 173 (2003).

⁷M. R. Overholt and S. B. Pope, "Direct numerical simulation of a passive scalar with imposed mean gradient in isotropic turbulence," *Phys. Fluids* **8**, 3128 (1996).

⁸P. A. O'Gorman and D. I. Pullin, "The velocity-scalar cross spectrum of stretched spiral vortices," *Phys. Fluids* **15**, 280 (2003).

⁹P. A. O'Gorman and D. I. Pullin, "Effect of Schmidt number on the velocity-scalar cospectrum in isotropic turbulence with a mean scalar gradient," *J. Fluid Mech.* **532**, 111 (2005).

¹⁰W. J. T. Bos, H. Touil, L. Shao, and J.-P. Bertoglio, "On the behavior of the velocity-scalar cross correlation spectrum in the inertial range," *Phys. Fluids* **16**, 3818 (2004).

¹¹W. J. T. Bos, H. Touil, and J.-P. Bertoglio, "Reynolds number dependency of the scalar flux spectrum in isotropic turbulence with a uniform scalar gradient," *Phys. Fluids* **17**, 125108 (2005).

¹²W. J. T. Bos and J.-P. Bertoglio, "Inertial range scaling of scalar flux spectra in uniformly sheared turbulence," *Phys. Fluids* **19**, 025104 (2007).

¹³Y. Sakai, K. Uchida, T. Kubo, and K. Nagata, "Statistical features of scalar flux in a high-Schmidt-number turbulent jet," in *Proceedings of the IUTAM Symposium 2006: Computational Physics and New Perspectives in Turbulence*, Nagoya (Springer, New York, 2006).

¹⁴Y. Kaneda and K. Yoshida, "Small-scale anisotropy in stably stratified turbulence," *New J. Phys.* **6**, 34 (2004).

¹⁵T. Gotoh, D. Fukayama, and T. Nakano, "Velocity field statistics in homogeneous steady turbulence obtained using a high-resolution direct numerical simulation," *Phys. Fluids* **14**, 1065 (2002).

¹⁶Y. Kaneda, T. Ishihara, M. Yokokawa, K. Itakura, and A. Uno, "Energy dissipation rate and energy spectrum in high resolution direct numerical simulations of turbulence in a periodic box," *Phys. Fluids* **15**, L21 (2003).

¹⁷T. Watanabe and T. Gotoh, "Intermittency, field structure and accuracy of DNS in a passive scalar turbulence," in *Proceedings of the IUTAM Symposium on Elementary Vortices and Coherent Structures: Significance in Turbulence Dynamics* (Springer, Dordrecht, 2006), p. 171.

¹⁸T. Watanabe and T. Gotoh, "Inertial-range intermittency and accuracy of direct numerical simulation of turbulence and passive scalar turbulence," *J. Fluid Mech.* **590**, 117 (2007).

¹⁹P. K. Yeung, D. A. Donzis, and K. R. Sreenivasan, "High-Reynolds-number simulation of turbulent mixing," *Phys. Fluids* **17**, 081703 (2005).

²⁰T. Watanabe and T. Gotoh, "Intermittency in passive scalar turbulence under the uniform mean scalar gradient," *Phys. Fluids* **18**, 058105 (2006).

²¹T. Watanabe and T. Gotoh, "Statistics of a passive scalar in homogeneous turbulence," *New J. Phys.* **6**, 40 (2004).

²²K. R. Sreenivasan, "The passive scalar spectrum and the Obukhov-Corrsin constant," *Phys. Fluids* **8**, 189 (1996).

²³Y. Tsuji, "Intermittency effect on energy spectrum in high-Reynolds number turbulence," *Phys. Fluids* **16**, L43 (2004).

²⁴T. Gotoh and D. Fukayama, "Pressure spectrum in homogeneous turbulence," *Phys. Rev. Lett.* **86**, 3775 (2001).